

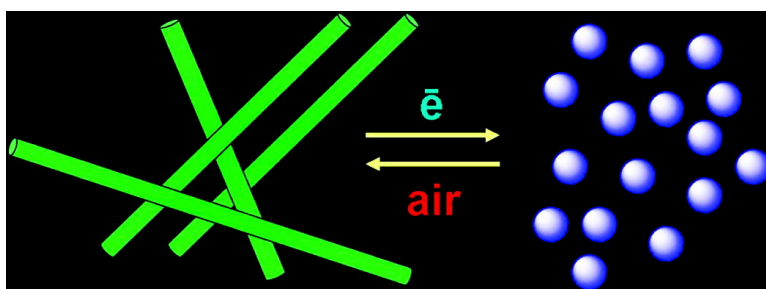
Communication

## Control over Self-Assembly through Reversible Charging of the Aromatic Building Blocks in Photofunctional Supramolecular Fibers

Jonathan Baram, Elijah Shirman, Netanel Ben-Shitrit, Alona Ustinov, Haim Weissman, Iddo Pinkas, Sharon G. Wolf, and Boris Rybtchinski

*J. Am. Chem. Soc.*, **2008**, 130 (45), 14966-14967 • DOI: 10.1021/ja807027w • Publication Date (Web): 17 October 2008

Downloaded from <http://pubs.acs.org> on February 8, 2009



### More About This Article

Additional resources and features associated with this article are available within the HTML version:

- Supporting Information
- Access to high resolution figures
- Links to articles and content related to this article
- Copyright permission to reproduce figures and/or text from this article

[View the Full Text HTML](#)

## Control over Self-Assembly through Reversible Charging of the Aromatic Building Blocks in Photofunctional Supramolecular Fibers

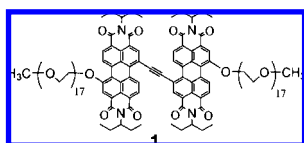
Jonathan Baram,<sup>†</sup> Elijah Shirman,<sup>†</sup> Netanel Ben-Shitrit,<sup>†</sup> Alona Ustinov,<sup>†</sup> Haim Weissman,<sup>†</sup> Iddo Pinkas,<sup>‡</sup> Sharon G. Wolf,<sup>§</sup> and Boris Rybtchinski\*<sup>†</sup>

Departments of Organic Chemistry, Plant Sciences, and Chemical Research Support, Weizmann Institute of Science, Rehovot 76100, Israel

Received September 4, 2008; E-mail: boris.rybtchinski@weizmann.ac.il

One of the main challenges in the field of supramolecular chemistry is creating adaptive systems, whose structure and function can be reversibly controlled in situ.<sup>1</sup> Solution-phase self-assembly of nanoscale systems built from stacked aromatic molecules bear great potential for creation of functional arrays.<sup>2</sup> It can be envisaged that in such systems charging of an aromatic primary building block will alter both morphology and function. Furthermore, reversible charging can result in turning on and off different structure/function modes based on a single molecular system. Herein we report on self-assembled photofunctional fibers, in which interactions between aromatic monomers can be attenuated through their reduction to anionic species that causes fiber fission. Oxidation with air restores the fibers. The sequence represents reversible supramolecular depolymerization–polymerization in situ and is accompanied by a reversible switching of photofunction.

To create a self-assembling motif based on hydrophobic interactions, we prepared amphiphilic compound **1** that has a large rigid aromatic core constructed from two strongly hydrophobic perylene diimide (PDI) units. The latter were functionalized with hydrophilic polyethylene glycol (PEG) groups (see Supporting Information for synthesis and characterization of **1**). PDIs are widely utilized dyes, and PDI-based systems have been shown to self-assemble in various media due to  $\pi$ -stacking.<sup>2,3</sup> PDI reduction in water gives stable radical anion and dianion species that can be converted to neutral PDI upon exposure to air,<sup>4</sup> allowing for reversible charging of PDI units.



In a water/THF mixture (4:1, v/v) compound **1** self-assembles into long fibers as evidenced by cryogenic transmission electron microscopy (cryo-TEM) (Figure 1). The fibers show a ribbonlike structure, and the fiber twisting from a narrow high-contrast edge ( $3.1 \pm 0.4$  nm) to a wider low-contrast face ( $8.8 \pm 1.1$  nm) is observed (Figure 1, black arrows). The length of the fibers reaches several micrometers. Occasional tightly packed domains of aligned fibers show fiber-to-fiber spacings of  $9.7 \pm 0.7$  nm (Figure 1A, blue arrows), which correspond to a high-contrast ordered aromatic core (responsible for fiber images in cryo-TEM) and low-contrast solvated PEGs (interfiber area). Notably, individual fibers show a segmented, “necklace” structure (Figure 1C inset and Figure S5). Such hierarchical structures with a segmented core are rare,<sup>5,6</sup> they

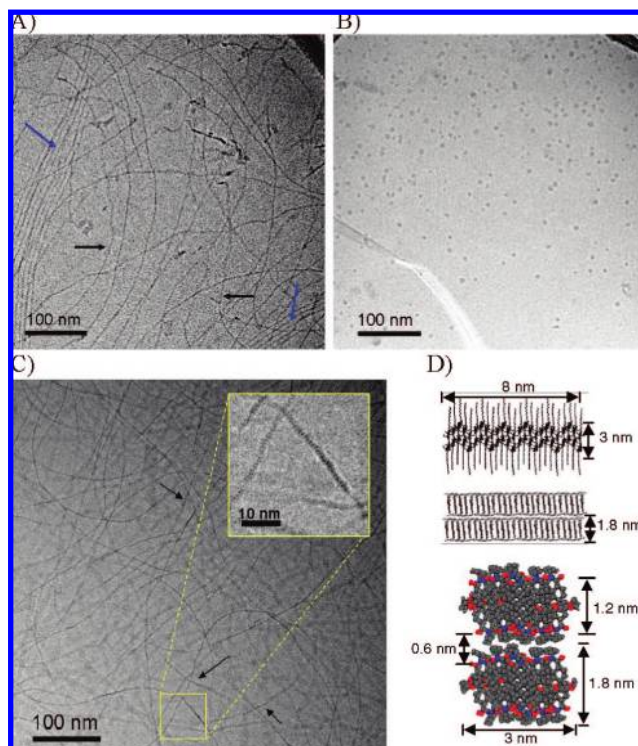


**Figure 1.** (A–C): Cryo-TEM images of **1** in water/THF mixture (4:1, v/v),  $1 \times 10^{-3}$  M. (A) Neutral system: black arrows, fiber twists; blue arrows, ordered domains. (B) Reduced system (the feature in the lower left part is due to a crack in the vitrified solvent). (C) The system after reduction, followed by oxidation with air. See Figure S5 for enlarged images. (D) Model of two fiber segments (molecular mechanics optimization, MM2 force field). From top to bottom: fiber cross-section, face, and edge (the latter is given at a larger scale) views. Hydrogen atoms (all structures) and PEG chains (bottom structure) were omitted for clarity. Enlarged model is given in Figure S12. The size of the PDI aromatic unit (N–N distance) is 1.2 nm, the intersegment distance is 0.6 nm. The intersegment space is filled with the ethylpropyl groups attached to the imide nitrogens.

were suggested to occur due to kinetic trapping.<sup>5</sup> Kinetically trapped wormlike structures assembled from disklike block copolymer micelles in water/THF mixtures have recently been observed.<sup>6</sup> Notably, the 1.8-nm segment periodicity (segment height of 1.2 nm and the low contrast intersegment spacing of 0.6 nm) is almost identical throughout all structures and corresponds well to the PDI dimensions. The possible molecular model is given in Figure 1D.

To corroborate cryo-TEM results, we performed a solution-phase small-angle X-ray scattering (SAXS) study on the self-assembled fibers of **1** using a high-flux synchrotron source. SAXS shows a pattern typical for rodlike structures (Figure S7).<sup>7</sup> The analysis of SAXS data (Figures S8–11) gives a radius of gyration  $R_g = 113$

<sup>†</sup> Department of Organic Chemistry.

<sup>‡</sup> Department of Plant Sciences.

<sup>§</sup> Department of Chemical Research Support.

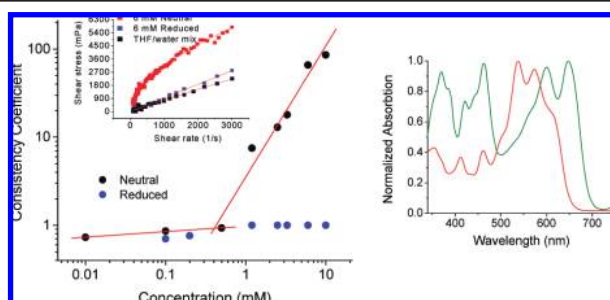


**Figure 2.** (Left) Concentration dependence of viscosity of **1** in water/THF (4:1) solution. Consistency coefficient  $K$  is obtained from the standard power law for shear dependent polymer solutions:  $\tau = K\theta^n$  where  $\tau$  is shear stress,  $\theta$  is shear rate, and  $K$  is a measure of viscosity independent of the shear rate. (Inset) An example of viscosity decrease upon reduction. Upon oxidation, viscosity returns to the initial levels. (Right) Normalized UV-vis spectra of disaggregated **1** in chloroform (red line) and self-assembled **1** in water/THF (4:1) solution (green line).

nm, cross-section diameter of 8.2 nm, persistence length of 27 nm, and contour length of 1.5  $\mu\text{m}$ , in agreement with cryo-TEM.

Rheological measurements (Figures 2, S3) of **1** in water/THF solution reveal shear thinning behavior, characteristic of linear polymers and wormlike micelles whose chains become untangled and oriented by flow.<sup>7</sup> Furthermore, distinctive switching of viscosity regimes upon increase in concentration (Figure 2) indicates the entanglement onset at  $\sim 10^{-3}$  M. UV-vis spectra of **1** in water/THF solution show a significant red shift in the PDI absorption in comparison to **1** in a disaggregated state (Figure 2), indicative of slipped stack formation (J-aggregates).<sup>3</sup>

Reduction of **1** in water/THF solution (8:2, v/v) with 10 equiv of sodium dithionite results in color change from green to blue, accompanied by a dramatic viscosity drop (Figure 2), indicating polymer fission. The fission is evidenced by cryo-TEM (Figure 1), revealing formation of spherical micelles,  $8.3 \pm 1.7$  nm in diameter. The reduced system was not sufficiently stable for SAXS studies. The reduced **1** gives rise to a broad absorption peak (450–700 nm) in UV-vis spectra, while EPR shows the presence of paramagnetic species (Figure S2). Electrochemistry of **1** in water/THF solution (Figure S3) reveals four one-electron reductions ( $-0.39$ ,  $-0.52$ ,  $-0.77$ , and  $-1.52$  V vs SCE), as expected for accommodation of two electrons by each PDI unit.<sup>4</sup> As sodium dithionite redox power does not allow reduction at potentials more negative than ca.  $-1.0$  V, it appears that **1** can be reduced to anionic states not exceeding trianion. The reduced **1** is stable for days when kept under inert atmosphere and protected from light. Upon exposure to air the reduced system is oxidized to neutral **1** within 1 h, restoring the supramolecular polymeric fibers as evidenced by cryo-TEM (Figure 1), and UV-vis (identical to the neutral system). The fibers retain a ribbonlike segmented structure, with high contrast width of  $3.1 \pm 0.3$  nm, and lower contrast width of  $9.1 \pm 1.1$  nm (Figure 1). The reduction/oxidation cycle can be repeated at least three times.

The apparent depolymerization of the fibers upon reduction is due to enhanced solvation of the anionic species and their mutual repulsion. Interestingly, air can be used to reverse the process. Oxygen-induced supramolecular polymerization is without precedent, bearing potential for a variety of applications. Evidently, orthogonal self-assembly propensities of the reduced and neutral PDIs make them advantageous building blocks for tunable multifunctional supramolecular systems.

As the fibers can undergo reversible fission, accompanied by a significant change in electronic properties, photofunction switching should be possible. Our preliminary femtosecond transient absorption studies reveal that in the neutral fibers the PDI excited-state peak shows multiexponential decay with time constants of 0.3, 4, and 300 ps (Figure S4). The contribution of the fast processes (0.3 and 4 ps) is dependent on the laser power, indicating that exciton annihilation takes place. This is typical of dye aggregates, where a high photon flux of a laser pulse causes multiple excitations enabling annihilation processes. It is a result of good exciton mobility in dye assemblies, creating a basis for light harvesting.<sup>2</sup> Disaggregated **1** (chloroform solution) does not show power-dependent behavior. Unlike the neutral fibers, the reduced form of **1** decomposes under laser light, most probably due to formation of highly energetic photoexcited anionic species. The fiber exciton dynamics is restored by oxidation with air. Thus, the fiber photofunction can be turned off and on using the reduction/oxidation sequence. Studies on the mechanism of the exciton relaxation and motion in the self-assembled **1** are currently underway.

In conclusion, we have prepared a novel photofunctional supramolecular polymer based on hydrophobic interactions. We have demonstrated that in situ control over hydrophobic self-assembly and photofunction of aromatic building blocks can be achieved through the reversible charging of aromatic systems. The latter allows for assembly/disassembly sequence akin to reversible depolymerization. We envisage that this methodology can be useful for the creation of adaptive multifunctional supramolecular systems.

**Acknowledgment.** This work was supported by grants from the Israel Science Foundation (Grant No. 917/06), and the Helen and Martin Kimmel Center for Molecular Design. The cryo-TEM studies were conducted at the Irving and Cherna Moskowitz Center for Nano and Bio-Nano Imaging (Weizmann Institute). Transient absorption studies were performed at the Dr. J. Trachtenberg laboratory for photobiology and photobiotechnology (Weizmann Institute) and were supported by a grant from Ms. S. Zuckermanof (Toronto, Canada). We thank Dr. L. Weiner for the assistance with EPR measurements, Prof. D. Milstein for the access to modeling software, Mr. J. Bullock for acquiring SAXS data, and Dr. N. Kampf for the assistance with rheological measurements. B.R. holds the Abraham and Jennie Fialkow Career Development Chair.

**Supporting Information Available:** Synthetic procedures, photo-physical, EPR, cryo-TEM, and SAXS data. This material is available free of charge via the Internet at <http://pubs.acs.org>.

## References

- (1) (a) Whitesides, G. M.; Grzybowski, B. *Science* **2002**, *295*, 2418–2421. (b) Lehn, J.-M. *Chem. Soc. Rev.* **2007**, *36*, 151–160.
- (2) (a) Hoeben, F. J. M.; Jonckheijm, P.; Meijer, E. W.; Schenning, A. P. H. J. *Chem. Rev.* **2005**, *105*, 1491–1546. (b) Elemans, J. A. A. W.; Van Hameren, R.; Nolte, R. J. M.; Rowan, A. E. *Adv. Mater.* **2006**, *18*, 1251–1266. (c) Ryu, J.-H.; Hong, D.-J.; Lee, M. *Chem. Commun.* **2008**, 1043–1054. (d) Zang, L.; Che, Y.; Moore, J. S. *Acc. Chem. Res.*, published online July 11, 2008. <http://dx.doi.org/10.1021/ar8000030w>.
- (3) (a) Würthner, F. *Chem. Commun.* **2004**, 1564–1579. (b) Wasielewski, M. R. *J. Org. Chem.* **2006**, *71*, 5051–5066.
- (4) Shirman, E.; Ustinov, A.; Ben-Shitrit, N.; Weissman, H.; Iron, M. A.; Cohen, R.; Rybtchinski, B. *J. Phys. Chem. B* **2008**, *112*, 8855–8858.
- (5) Jain, S.; Bates, F. S. *Macromolecules* **2004**, *37*, 1511–1523.
- (6) (a) Li, Z. B.; Kesselman, E.; Talmon, Y.; Hillmyer, M. A.; Lodge, T. P. *Science* **2004**, *306*, 98–101. (b) Cui, H. G.; Chen, Z. Y.; Zhong, S.; Wooley, K. L.; Pochan, D. J. *Science* **2007**, *317*, 647–650.
- (7) Dreiss, C. A. *Soft Matter* **2007**, *3*, 956–970.

JA807027W